Chinese Chemical Letters 33 (2022) 4405–4410

Contents lists available at ScienceDirect

Chinese Chemical Letters

journal homepage: www.elsevier.com/locate/cclet

Paper-based fluorescent devices for multifunctional assays: Biomarkers detection, inhibitors screening and chiral recognition

Wang Li[a,b], Xiaoyue Zhang[a,b], Siqi Chen[a,b], Yibing Ji[a,b,*], Ruijun Li[a,b,*]

[a] Department of Analytical Chemistry, China Pharmaceutical University, Nanjing 210009, China
[b] Key Laboratory of Drug Quality Control and Pharmacovigilance, Ministry of Education, Nanjing 210009, China

ARTICLE INFO

Article history:
Received 23 August 2021
Revised 7 October 2021
Accepted 11 December 2021
Available online 17 December 2021

Keywords:
Paper-based devices
Multifunctional
Xanthine
Inhibitor screening
Chiral recognition

ABSTRACT

The development of a single analytical platform with different functions is highly desirable but remains a challenge at present. Here, a paper-based device based on fluorescent carbon dots (CDs) functionalized paper/MnO_2 nanosheets (MnO_2 NS) hybrid devices (PCD/NS) was proposed for single-device multifunction applications. MnO_2 NS functioned as a fluorescence quencher of CDs and recognizer of H_2O_2 released from the oxidase catalyzed system. Fluorescence recovery would occur after the decomposition of MnO_2 NS induced by H_2O_2, by which a simple and effective strategy could be developed for fluorescence monitoring multiplex biological events. Xanthine (XA) sensing, xanthine oxidase (XOD) inhibitors screening analysis and chiral recognition of glucose enantiomers were performed on PCD/NS to investigate the multifunctional application of the paper-based device. By means of PCD/NS, XA could be determined in the range of 0.1–40 μmol/L with a low detection of limit of 0.06 μmol/L. The IC_{50} value of allopurinol, the model inhibitor of XOD, was sensitively detected to be 7.4 μmol/L. Glucose enantiomers were also recognized in terms of the specific fluorescence response to D-glucose. This work firstly presented a paper-based device capable of biomarkers detection, inhibitors screening and chiral recognition, which enlightened a promising strategy for the construction of multifunctional devices and hold the great potential application in clinical diagnosis and drug discovery.

Enzyme is a natural catalyst that takes part in the catalysis of almost all biochemical processes with high efficiency and specificity [1]. This arouses the considerable interest of researchers to engineer various ingenious enzymatic analytical devices, furnishing clinical diagnosis and biomedicine with sensitive and selective monitoring platforms [2]. Oxidase, the widely distributed enzyme in the human body, can catalyze the transformation of numerous metabolites (*e.g.*, glucose, cholesterol, choline, sarcosine) in the presence of oxygen, and induce the generation of hydrogen peroxide at the same time [3,4]. Monitoring oxidase catalyzed reactions is of ongoing interest for analytical science due to its significant role in early cancer diagnosis, drug discovery and evaluation of prognosis [5–7]. The method to identify and quantify the related biological events in an oxidase-mediated catalysis system is, therefore, the fundamental and central task of the monitoring work. Up until now, numerous strategies based on electrochemistry [8], chemiluminescence [9], and high-performance liquid chromatography [10], have been developed to achieve the signal readout in the oxidase-mediated catalytic systems. However, most of these approaches are rather limited on account of the necessities of complicated operations, skilled personnel and large instruments, which impede their widespread utilization in practical application. Therefore, simple, affordable and effective strategies are highly desirable and necessary.

Paper-based devices, a class of emerging analytical platforms, have drawn much attention owing to its advantages of simple operation, light weight and great biocompatibility [11–14]. As a universal substrate, the porous structure of the paper, along with an easily modifiable surface and a large surface-to-volume ratio [15–18], make it a splendid supporter for the incorporation of functional nanomaterials and a flexible platform for the development of elaborate analytical devices. Especially, a multifunctional analytical system relying on paper-based devices has received great concerns. Kamei's group achieved the automation of target analytes preconcentration, capture and signal amplification on a paper-based device [19]. Sahatiya *et al.* proposed a MoS_2/Cu_2S hybrid paper-based sensor that could be applied in sensing of humidity, temperature, breath, and ethanol adulter-

* Corresponding authors.
E-mail addresses: jiyibing@msn.com (Y. Ji), ccjlrj@cpu.edu.cn (R. Li).

https://doi.org/10.1016/j.cclet.2021.12.026
1001-8417/

ation [20]. Nevertheless, many problems need to be solved in the present stage. For instance, multiple modules were usually assembled onto paper surface to perform different functions, which would increase the complexity of the operation and add cost to the fabrication of multifunctional paper-based devices [21]. Multifunctional paper-based devices signify an advancement of paper-based assays, which also show promising prospects in the construction of flexible and portable multiparameter monitoring devices in the field of *in vitro* diagnosis (IVD). Thus, the development of novel strategies for engineering multifunctional paper-based devices with simple structures and low cost is necessary and significant.

Herein, a renovated multifunctional paper-based device for monitoring biological events of oxidase catalyzed reactions based on fluorescence "turn-on" sensing mode was proposed. The cellulose paper was functionalized with fluorescent carbon dots (CDs) as sensing element, and manganese dioxide nanosheets (MnO_2 NS) as fluorescence quencher and recognition element simultaneously, resulting in the CDs functionalized paper (PCD)/MnO_2 NS hybrid platform (PCD/NS). The quenched fluorescence of CDs on paper could be recovered after the decomposition of MnO_2 NS caused by H_2O_2 released from oxidase catalyzed reactions. The feasibility of PCD/NS was demonstrated by the implementation of xanthine (XA) sensing, inhibitors screening analysis of xanthine oxidase (XOD) and chiral recognition of D-/L-glucose on a single paper-based device. To our best knowledge, such a multifunctional paper-based device enabling biomarkers detection, inhibitors screening and chiral discrimination has never been explored, and it provides a flexible and powerful platform for monitoring multiple biological events of oxidase catalyzed reactions.

The amine-terminated CDs were synthesized according to the previous report with some modifications [22]. Briefly, citric acid (5.260 g) and ethanediamine (2512.5 μL) were dissolved into 50 mL water. Then, the transparent solution was sealed into a poly (tetrafluoroethylene) (Teflon)-lined autoclave for hydrothermal reaction. After 6-h heating at 130 °C and cooling to room temperature, the dark yellow colored CDs solution was obtained. Finally, the CDs solution was kept at 4 °C before use.

For the synthesis of MnO_2 NS, a simple and time-efficient method was adopted following literature reports with minor modifications [23]. Firstly, 3-morpholinopropanesulfonic acid (MOPS, 209.3 mg) and $KMnO_4$ (15.8 mg) were added into 10 mL water. The mixture was then sonicated for 30 min at room temperature. After ultrasonication, the resulting solution was centrifuged at 12,000 rpm for 5 min to collect MnO_2 precipitate. The precipitate was washed with ultrapure water for several times. At last, the as-synthesized MnO_2 NS were dispersed in ultrapure water with a concentration of 486 μmol/L ($\varepsilon = 9.6 \times 10^{-3}$ L mol^{-1} cm^{-1} at 380 nm [24]) for the subsequent investigation.

The PCD/NS was fabricated by the covalent immobilization of CDs and followed the deposition of MnO_2 NS on paper (Scheme 1A). The CDs were grafted on paper by Schiff base chemistry (Fig. S1 in Supporting information), to obtain PCD, the fluorescence sensing substrate of the proposed paper-based devices. To begin with, the filter paper was cut into paper discs with a diameter of 6 mm and activated with HCl (0.2 mol/L) for 30 min. The resulted paper discs were then immersed into periodic acid (34 mg/mL) for two hours, by which aldehyde groups were generated on the paper surface. Next, the paper discs with aldehyde groups were soaked into the CDs solution with $NaCNBH_3$ (4 mg/mL) for 8 min (Fig. S2A in Supporting information), followed by thoroughly washing three times with ultrapure water to remove the CDs adsorbed by physical adsorption. After that, MnO_2 NS was coated onto the surface of PCD by through a direct deposition method with 243 μmol/L of MnO_2 NS for 2 h (Fig. S2B in Supporting information), and then the obtained PCD/NS was rinsed 3 times with ultrapure water. Finally, the PCD/NS was dried and stored at room temperature before to use.

For fluorescence "turn-on" sensing of XA, PCD/NS was incubated with the oxidase catalyzed reaction system containing XOD (1 U/mL, 200 μL), NaAc-HAc buffer (0.2 mol/L, pH 7.0) and XA with various concentrations at the final volume of 1 mL for 24 min at room temperature. Then, PCD/NS was taken out and dried. Next, for the acquisition of fluorescence spectra, PCD/NS was embedded in a homemade holder (Fig. S3 in Supporting information) and 8 μL NaAc-HAc buffer (0.2 mol/L, pH 7.0) was added to saturate the paper. The fluorescence spectra were recorded with the excitation wavelength at 370 nm. For the detection of XA in real samples, the human serum was diluted to 10 times [25], and XA was added into the serum and detected with the identical procedures.

Allopurinol was selected as the model inhibitor for XOD inhibition assay based on the proposed PCD/NS platform. Different concentrations of allopurinol were added into the oxidase catalyzed reaction system with XA (40 μmol/L), XOD (25 U/L), and NaAc-HAc buffer (0.2 mol/L, pH 7.0). The fluorescence spectra were measured after incubation for 40 min at room temperature.

The chiral discrimination of glucose enantiomers by the PCD/NS was performed as the procedures followed. PCD/NS was incubated with the reaction solution of D-glucose (D-Glu) (80 μmol/L), glucose oxidase (GOD) (100 U/mL) and phosphate buffer (0.01 mol/L, pH 6.0) for 24 min at room temperature. Meanwhile, the fluorescent response of PCD/NS to L-glucose (L-Glu) was observed by conducting identical measurement.

The amine-terminated CDs were prepared by a facile hydrothermal method using citric acid as a carbon source and ethylenediamine as modification reagents. The transmission electron microscope (TEM) images (Fig. 1A) presented the spherical morphology of the as-prepared amine-terminated CDs, with the diameter distribution in the range of 3.5 nm to 5.5 nm (Fig. S4 in Supporting information). High resolution TEM image showed well-resolved lattice structures with a spacing of 0.21 nm (Fig. 1A), which was corresponding to the (100) facet of graphite and unveiled a graphite-like structure. FT-IR was performed to identify the surface functional groups. As shown in Fig. 1B, the absorption peaks at 3371 cm^{-1} and 1568 cm^{-1} were attributed to the stretching and bending vibrations of N−H respectively, which demonstrated the existence of amine on the surface of the CDs. Besides, the other characteristic peaks in the spectrum could be assigned to the stretching vibrations of C=O (1633 cm^{-1}) and O−H (3053 cm^{-1}), bending vibration of C−N (1269 cm^{-1}). The optical property of the as-prepared CDs was investigated with UV–vis absorption and fluorescence spectra. As shown in Fig. 1C, the strong characteristic absorption bands at 344 nm were attributed to the n-π^* transition of C=O. A bright blue fluorescence of the CDs under a 365 nm UV lamp can be observed by naked eyes, and the fluorescence spectra suggested an emission peak located at 440 nm upon excited 360 nm (Fig. 1C).

The MnO_2 NS was synthesized here by a redox reaction between MOPS and $KMnO_4$. The TEM image (Fig. 1D) of the prepared MnO_2 NS showed a typical two dimensional sheet-like morphology with some wrinkles, along with the ultrathin and transparent structure. Additionally, zeta potential measurement (Fig. S5 in Supporting information) revealed that the obtained MnO_2 NS were negatively charged (−22.7 mV) [26]. The XPS exhibited characteristic peaks centered at 653.2 eV (Mn $2p_{1/2}$) and 641.5 eV (Mn $2p_{3/2}$) (Fig. 1E), which fully confirmed the successful synthesis of MnO_2 NS [27]. More importantly, as exhibited in Fig. 1F, the MnO_2 NS displayed a wide UV–vis absorption band ranging from 240 nm to 700 nm, overlapping well with the excitation and emission spectra of CDs.

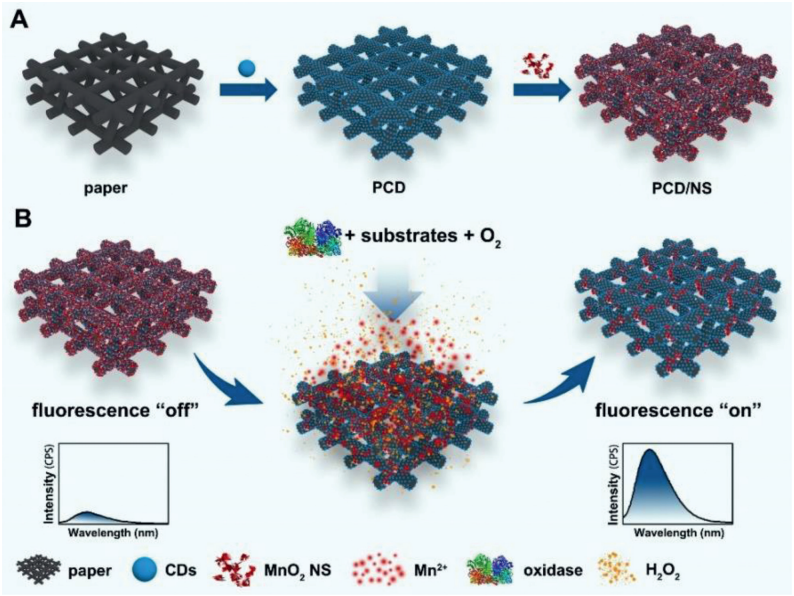

Scheme 1. Schematic illustration of the fabrication of PCD/NS (A) and fluorescence sensing principle of PCD/NS for monitoring oxidase catalyzed reactions (B).

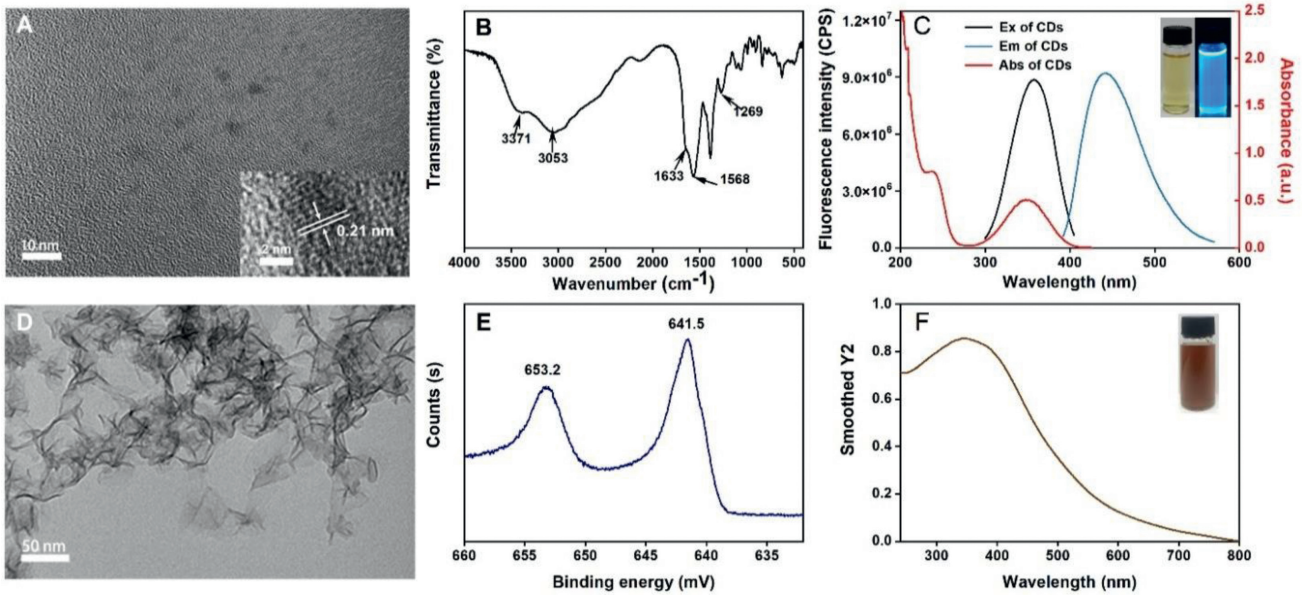

Fig. 1. (A) TEM images of CDs (inset: high magnification TEM image of the CDs). (B) FT-IR spectrum of the CDs. (C) UV–vis absorption spectrum, fluorescence excitation and emission spectra of the CDs. Inset: the images of CDs solution under daylight and 365 nm UV lamp. TEM images (D), XPS spectrum (E) and UV–vis absorption spectrum (F) of MnO_2 NS.

PCD/NS were fabricated by the covalent immobilization of CDs on cellulose paper, followed by the deposition of MnO_2 NS. The cellulose paper was initially immersed in hydrochloric acid to activate the hydroxy groups and remove the additives [28]. Then, a multitude of aldehyde groups were generated on the paper through the oxidation reaction between periodic acid and 1,2-dihydroxyl (glycol) groups of glucose units (Fig. S1). Next, the oxidated paper was bathed in a CDs solution, where the Schiff base reaction between -CHO exposed on paper fiber and -NH_2 on the surface of CDs could be initiated. Since the formed Schiff base was unstable in an aqueous solution, $NaCNBH_3$ was added into the reaction solution to reduce the C=N bond [29]. At last, the PCD were thoroughly washed with water to remove the loosely immobilized CDs which were anchored on paper by physical adsorption. Due to the relatively small particle size of CDs, the scanning electron microscopy (SEM) images showed no distinct difference between bare paper (Fig. 2A) and PCD (Fig. 2B). However, the fluorescence spectra revealed that PCD showed much higher fluorescence intensity over the bare paper, confirming the successful immobilization of CDs on paper (Fig. S6 in Supporting information). The distribution of CDs on paper was also examined by the detection of fluorescence intensity of 30 sites from different PCD, and the result showed the CDs were uniformly immobilized on paper (Fig. S7 in Supporting information). To offer a more stable fluorescence signal and a more favorable reproducibility of the proposed paper-based platform, the CDs were grafted onto the surface of the paper by a covalent modification strategy. As illustrated in Fig. S8 (Supporting information), the fluorescence intensity of PCD prepared by direct physical adsorption was much lower than its counterpart, and the CDs could be removed from the paper after a simple washing pro-

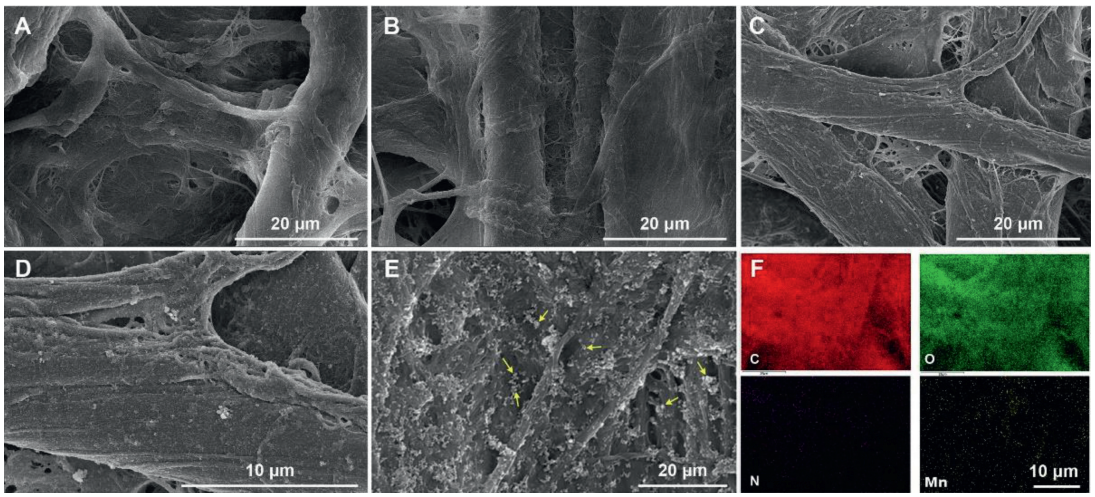

Fig. 2. SEM images of paper (A), PCD (B), PCD/NS (C-E) with different magnifications and mapping images of PCD/NS (F). MnO_2 NS deposited on PCD were indicated with yellow arrows (E). The scale bar is 10 μm (F).

cess. MnO_2 NS, as a recognizer and a fluorescence quencher, was deposited on PCD, for construction of the multifunctional paper-based devices. The hydroxyl groups on the surface of MnO_2 NS would strongly interact with amino groups of CDs and hydroxyl groups of cellulose paper substrate through electrostatic interaction and hydrogen bond, leading to a stable adsorption of MnO_2 NS on PCD. SEM and mapping images (Figs. 2C-F) of PCD/NS suggested that there was a uniform distribution of MnO_2 NS in the fiber of PCD. These results demonstrated that the CDs and MnO_2 NS were successfully introduced onto paper, which laid the foundation of the fluorescence sensing system of the proposed paper-based device.

The proposed paper-based device enables the multiple functions of biomarkers detection, inhibitor screening and chiral discrimination and so forth, which are based on the H_2O_2-released oxidase reaction system. As illustrated in Scheme 1B, MnO_2 NS, the fluorescence quencher of CDs, would be decomposed by H_2O_2 released from the oxidase catalyzed reaction, resulting in the occurrence of fluorescence recovery, which could be monitored by fluorescence measurements. In Fig. 3A, after the deposition of MnO_2 NS, the fluorescence of the paper-based platform drastically weakened, and the fluorescence distribution of PCD/NS was also satisfactory (Fig. S7). According to the previous reports, the inner filter effect (IFE) or Förster resonance energy transfer (FRET) is deemed to be the main cause of the MnO_2 NS induced fluorescence quenching of CDs [30]. To give a detailed explanation for that, the fluorescence lifetime of CDs in the absence and presence of MnO_2 NS were measured respectively. As shown in Fig. S9A (Supporting information), the lifetime of the CDs without MnO_2 NS was 16.3 ns, which was nearly the same as that of the mixture of both (15.7 ns). Therefore, it excluded the existence of FRET, which usually occurred in accompany with the change of fluorescence lifetime [31]. Apart from this, the UV–vis spectra denied the possibility of a static quenching mechanism, because there is no new peak in the absorption band of the mixture of CDs and MnO_2 NS (Fig. S9B in Supporting information) [31]. Thus, IFE is principally responsible for the quenched fluorescence of CDs, because the UV–vis absorption spectrum of MnO_2 NS overlapped well with the excitation spectrum of CDs (Fig. S9C in Supporting information). Further, the response of PCD/NS towards H_2O_2 was also investigated. In Fig. 3A, the introduction of H_2O_2 yielded the recovered fluorescence of PCD/NS apparently, which was resulted from the H_2O_2 induced MnO_2 NS degradation to Mn^{2+} [30], evidencing the capability of the proposed paper-based device as an effective tool for monitoring the oxidase-related reactions.

The well-constructed PCD/NS offered the function as a sensing platform for the quantification of the oxidase-catalyzed biomarkers, which could be catalyzed by the corresponding oxidase and then trigger the generation of H_2O_2. Accordingly, these biomarkers are capable of being detected by the fluorescence "turn-on" strategy. As a proof-of-concept, XA was chosen as a target to give a verification of the application of PCD/NS in biomarkers detection. XA plays a vital role in purine nucleotide metabolism and correlates with diagnose of hyperuricemia, gout, xanthinuria and so forth [32]. Therefore, it is significant to develop a simple, low-cost and sensitive method for quantification of XA. To achieve the efficient fluorescence sensing, the effect of incubation time and the concentration of XOD were investigated here. As shown in Fig. S10A (Supporting information), with the increment of the incubation time, the recovered fluorescence of PCD/NS increased quickly, and then leveled off after 24 min. Then the concentration of XOD used in the sensing process was also studied. From Fig. S10B (Supporting information), it was notable that 0.2 U/mL of XOD was sufficient for the fluorescence sensing process. Therefore, the incubation time of 24 min and 0.2 U/mL of XOD were selected as the optimal conditions for sensing of XA with PCD/NS.

The sensing performance of the PCD/NS for detection of XA was then investigated under the optimal conditions. As depicted in Fig. 3B, the fluorescence of PCD/NS gradually restored as the increase of the concentration of XA. A well plotted linear relationship between F_1/F_0 of PCD/NS and the concentration of XA in the scope of 0.1–40 μmol/L was shown in Fig. 3C, giving the linear equation expressed as $F_1/F_0 = 0.1329C_{XA} + 1.2148$ ($R^2 = 0.99705$). F_0 and F_1 were the fluorescence intensity of PCD/NS in the absence and presence of XA. The LOD was calculated to be 0.06 μmol/L based on $3\sigma/k$ ("σ" represents the standard deviation of blank determination, "k" represents the slope of calibration curve), which was lower than most of the previous reports (Table S1 in Supporting information) and verified that the proposed PCD/NS could be a sensitive and effective platform for biomarkers detection.

The selectivity of PCD/NS for sensing of XA was evaluated by investigating the fluorescence response to the potential interferences. As displayed in Fig. S11 (Supporting information), the fluorescence recovery of the PCD/NS towards interfering species were negligible, confirming good specificity of the XA sensing system. The repeatability of PCD/NS was also tested, PCD/NS fabricated from the same batch and different batches were utilized for sens-

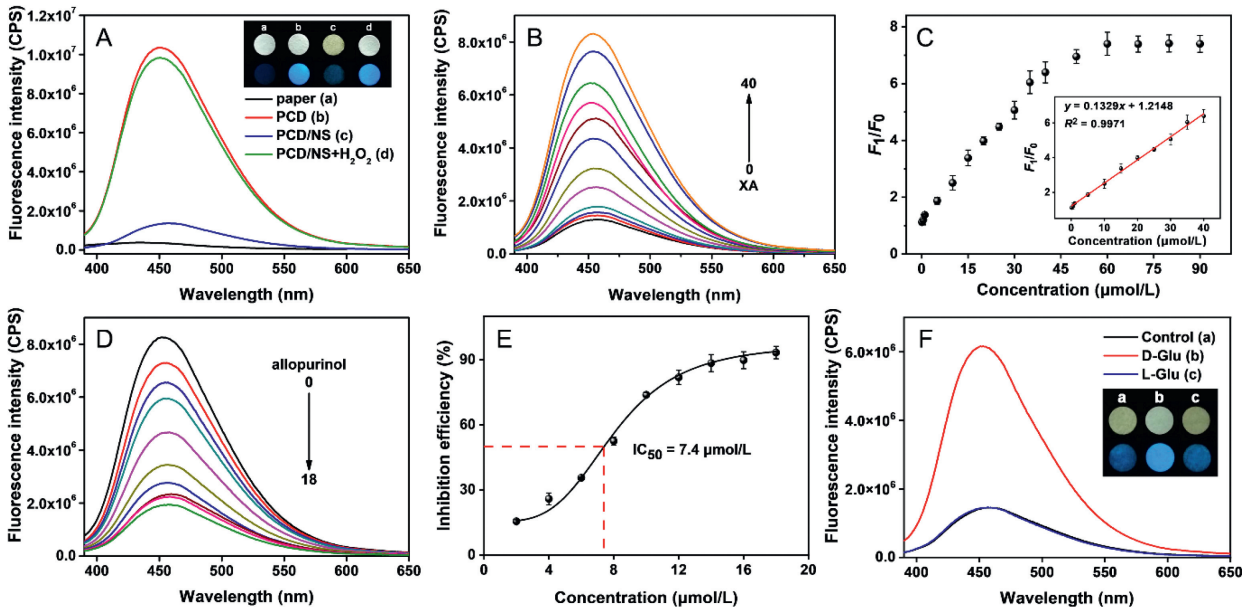

Fig. 3. (A) Fluorescence spectra of paper, PCD, PCD/NS and PCD/NS after the incubation with H_2O_2 (90 μmol/L). Inset: photographs and fluorescence images of paper (a), PCD (b), PCD/NS (c) and PCD/NS+H_2O_2 (d). (B) Fluorescence spectra of PCD/NS after being incubated with different concentrations of XA (from bottom to top: 0, 0.1, 0.5, 1, 5, 10, 15, 20, 25, 30, 35, 40 μmol/L). (C) The relationship between F_1/F_0 and XA concentrations from 0.1 μmol/L to 90 μmol/L. Inset: the calibration curve of the concentration of XA *versus* F_1/F_0 from 0.1 to 40 μmol/L ($n = 3$). (D) Fluorescence spectra of PCD/NS with different concentrations of allopurinol (from top to bottom: 0, 2, 4, 6, 8, 10, 12, 14, 16, 18 μmol/L). (E) The relationship between inhibition efficiency and the concentration of allopurinol from 2 μmol/L to 18 μmol/L ($C_{XA} = 40$ μmol/L, $C_{XOD} = 25$ U/L, $n = 3$). (F) Fluorescence spectra of PCD/NS after the incubation with blank solution, D-Glu, and L-Glu, respectively. Inset: photographs of PCD/NS+blank solution (a), PCD/NS+D-Glu (b), and PCD/NS+L-Glu (c) under visible light (top) and 365 nm UV lamp (bottom).

ing of XA with varying concentrations (5 μmol/L, 20 μmol/L and 40 μmol/L). The results of intra- and inter-assay ($n = 5$) gave the low RSD of 4.1% and 5.1%, respectively. That result reflected the proposed PCD/NS possessed good repeatability. In addition, stability made great sense in the practical application of the paper-based devices, and thereby, the storage stability was examined by the measurement of the sensitivity of PCD/NS on the sensing of XA. The results suggested a good stability of PCD/NS since its response towards XA had no distinct discrepancy after 120 days of storage at ambient temperature (Fig. S12 in Supporting information). The feasibility of the proposed paper-based devices was further investigated by detection XA in spiked serum samples. The results (Table S2 in Supporting information) showed that good recoveries in the range of 97.62%–105.2% were obtained and the RSD was less than 5.1%, which demonstrated the practicability of PCD/NS in the assay of biological samples. Therefore, it was exemplified by the XA sensing with PCD/NS that the proposed novel paper-based device displayed a promising prospect for the detection of the oxidase-catalyzed biomarkers.

XOD is a vital enzyme involving in purine metabolism and exists extensively within mammalian tissues [33]. Nevertheless, high levels of XOD may also lead to the occurrence of hyperuricemia and gout [34]. It is therefore essential to develop analytical strategies for the screening of XOD inhibitors. Here, the PCD/NS was evaluated as a novel platform for the inhibitors screening analysis of XOD. Allopurinol, a clinical drug for the treatment of gout [35], was selected as the model inhibitor of XOD for the following investigation. The fluorescence quantitative analysis of allopurinol's inhibition effect was achieved by the calculation of inhibition efficiency (IE) expressed as follows (Eq. 1):

$$\text{Inhibition efficiency\%} = \frac{F_1 - F_2}{F_1 - F_0} \times 100\% \quad (1)$$

where F_2 and F_1 referred to the fluorescence intensity of PCD/NS (in the presence of XA and XOD) with and without inhibitor, and F_0 referred to the fluorescence intensity of PCD/NS in the absence of both XA and inhibitor. (F_1-F_0) reflected the intact XOD activity, while (F_1-F_2) reflected the inhibited XOD activity by allopurinol. As displayed in Fig. 3D, the fluorescence recovery was distinctly restrained with the increase of the concentration of allopurinol. The attenuated fluorescence recovery could be attributed to the decrease of released H_2O_2 resulting from the inhibited XOD activity. IC_{50} value, the concentration of inhibitor when IE reached a level of 50%, was employed to evaluate the efficacy of inhibitor. By plotting IE and the concentration of allopurinol (Fig. 3E), the IC_{50} was calculated to be 7.4 μmol/L, which was lower than the previous reported strategies [34,36], suggesting a higher sensitivity of the PCD/NS for XOD inhibitors screening. The results proved that PCD/NS hold the potential of acting as a simple and sensitive tool for inhibitors screening and further, drug discovery for the oxidase related diseases.

Discrimination of enantiomers is of paramount significance for biomedical and pharmaceutical research all the time due to extensive involvement of chiral molecules in physiological process. Up until now, a number of strategies on the basis of chromatographic technologies relying on sophisticated instructments and operations have been developed for chiral identification [37–39]. However, reports on enantioselective recognition based on simple and portable paper-based device have been scarce [40]. In the present work, the proposed multifunctional paper-based device was further employed for the recognition of glucose enantiomers, by means of that GOD was capable of specifically catalyzing D-glucose rather than L-glucose to produce hydrogen peroxide. As illustrated in Fig. 3F, PCD/NS presented a considerable fluorescence recovery towards D-glucose, and yet exhibited little response to L-glucose and other monosaccharides (Fig. S13 in Supporting information). Meanwhile, the chiral discrimination based on PCD/NS could be also visualized under daylight or UV lamp (inset in Fig. 3F). Moreover, the determination of D-glucose in human serum using PCD/NS also gave good consistency with clinical glucose detection kits (Table S3 in Supporting information). In terms of the remarkable performance of PCD/NS, it was illuminated that

enantiomers discrimination based on paper-based device was an alternative strategy for analysis of chiral molecules in the future research.

In conclusion, a multifunctional paper-based device (PCD/NS) was designed and fabricated in this work. The proposed PCD/NS presented a sensitive response to the generated H_2O_2 in the oxidase catalyzed reactions, by which for the first time, biomarkers detection, inhibitors screening analysis and chiral discrimination were achieved on a single paper-based device. The analytical performance of PCD/NS was investigated by the detection of XA and XOD inhibitors screening, respectively. PCD/NS enabled the sensitive and selective detection of XA with a low LOD of 0.06 μmol/L, and exhibited favorable repeatability, stability and practicability. The inhibitors screening analysis of XOD was also performed on PCD/NS, which gave the low IC_{50} of 7.4 μmol/L. Further, the PCD/NS was developed as a novel chiral recognition platform with enantioselective response towards glucose enantiomers. PCD/NS presented a considerable fluorescence recovery towards D-glucose, and yet exhibited little response to L-glucose. Besides these, the proposed versatile paper-based device is also anticipated to be applied in other oxidase-related or biologically produced H_2O_2 system, realizing more applications in clinical diagnosis and biochemical analysis.

Declaration of competing interest

The authors declare no competing financial interest.

Acknowledgments

This work was financially supported by the National Natural Science Foundation of China (No. 21804141) and "Double First-Class University" Project (Nos. CPU2018GY07 and CPU2018GY21).

Supplementary materials

Supplementary material associated with this article can be found, in the online version, at doi:10.1016/j.cclet.2021.12.026.

References

[1] X. Yan, T.Y. Hu, L. Wang, et al., Biosens. Bioelectron. 79 (2016) 922–929.
[2] Z.Y. Qu, N. Li, W.D. Na, et al., Talanta 192 (2019) 61–68.
[3] N. Li, A. Than, X.W. Wang, et al., ACS Nano 10 (2016) 3622–3629.
[4] E. Ito, S. Watabe, M. Morikawa, et al., Method Enzymol. 526 (2013) 135–143.
[5] V. Thiagarajan, S. Madhurantakam, S. Sethuraman, et al., J. Colloid Interface Sci. 462 (2016) 334–340.
[6] L.H. Fu, C. Qi, J. Lin, et al., Chem. Soc. Rev. 47 (2018) 6454–6472.
[7] E. Garattini, M. Terao, Drug Metab. Rev. 43 (2011) 374–386.
[8] Z.P. Zhang, J. Hao, T.F. Xiao, et al., Analyst 140 (2015) 5039–5047.
[9] X. Jie, H.M. Yang, M. Wang, et al., Angew. Chem. Int. Ed. 56 (2017) 14596–14601.
[10] D.Q. Li, J. Zhao, S.P. Li, J. Chromatogr. A 1345 (2014) 50–56.
[11] L. Li, X.X. Zheng, Y.Z. Huang, et al., Anal. Chem. 90 (2018) 13882–13890.
[12] J.R. Zhou, B.W. Li, A.J. Qi, et al., Sens. Actuators B: Chem. 305 (2020) 127462.
[13] J. Qi, B.W. Li, X.Y. Wang, et al., Anal. Chem. 90 (2018) 11827–11834.
[14] M. Xiao, Z.G. Liu, N.X. Xu, et al., ACS Sens. 5 (2020) 870–878.
[15] S.M. Wang, L. Ge, L. Li, et al., Biosens. Bioelectron. 50 (2013) 262–268.
[16] L.M. Wang, F.W. Zhu, Y.Q. Zhu, et al., ACS Sens. 4 (2019) 3283–3290.
[17] X.R. Guo, J.Z. Huang, Y.B. Wei, et al., J. Hazard. Mater. 381 (2020) 120969.
[18] M. Na, S.P. Zhang, J.J. Liu, et al., J. Hazard. Mater. 386 (2020) 121956.
[19] D.W. Bradbury, M. Azimi, A.J. Diaz, et al., Anal. Chem. 91 (2019) 12046–12054.
[20] P. Sahatiya, A. Kadu, H. Gupta, et al., ACS Appl. Mater. Interfaces 10 (2018) 9048–9059.
[21] V. Soum, S. Park, A.I. Brilian, et al., Micromachines (Basel) 10 (2019) 516.
[22] S.J. Zhu, Q.N. Meng, L. Wang, et al., Angew. Chem. Int. Ed. 52 (2013) 3953–3957.
[23] L. Fu, Y. Du, Z. Zhang, et al., Microchim. Acta 186 (2019) 491.
[24] K. Kai, Y. Yoshida, H. Kageyama, et al., J. Am. Chem. Soc. 130 (2008) 15938–15943.
[25] Y.S. Ma, Y. Cen, M. Sohail, et al., ACS Appl. Mater. Interfaces 9 (2017) 33011–33019.
[26] H. Wang, X. Na, S. Liu, et al., Talanta 201 (2019) 388–396.
[27] D.Q. Fan, C.S. Shang, W.L. Gu, et al., ACS Appl. Mater. Interfaces 9 (2017) 25870–25877.
[28] B.W. Li, Z. Zhang, J. Qi, et al., ACS Sens. 2 (2017) 243–250.
[29] W. Hong, S.G. Jeong, G. Shim, et al., Biotechnol Bioproc. E 23 (2018) 686–692.
[30] J. Chen, H.M. Meng, Y. Tian, et al., Nanoscale Horiz. 4 (2019) 321–338.
[31] F.L. Zu, F.Y. Yan, Z.J. Bai, et al., Microchim. Acta 184 (2017) 1899–1914.
[32] X.X. Wang, Q. Wu, Z. Shan, et al., Biosens. Bioelectron. 26 (2011) 3614–3619.
[33] Y.J. Wang, G.W. Zhang, J.H. Pan, et al., J. Agric. Food. Chem. 63 (2015) 526–534.
[34] L. Chang, X.Y. Yao, Q. Liu, et al., Talanta 183 (2018) 83–88.
[35] J. Wang, D.F. Shi, M.Z. Zheng, et al., J. Sep. Sci. 40 (2017) 4160–4167.
[36] D.D. Tang, J.Y. Zhang, R.X. Zhou, et al., Nanoscale 10 (2018) 8477–8482.
[37] Y.Y. Wang, S.Q. Zhuo, J.W. Hou, et al., ACS Appl. Mater. Interfaces 11 (2019) 48363–48369.
[38] G. D'Orazio, Trends Anal. Chem. 125 (2020) 115832.
[39] S.M. Xie, X.X. Chen, J.H. Zhang, et al., Trends Anal. Chem. 124 (2020) 115808.
[40] F. Copur, N. Bekar, E. Zor, et al., Sens. Actuators B: Chem. 279 (2019) 305–312.